Optimal energy management for a jaw crushing process in deep mines

B.P. Numbi[a,*], J. Zhang[a,b], X. Xia[a]

[a] *Department of Electrical, Electronic and Computer Engineering, University of Pretoria, Pretoria 0002, South Africa*
[b] *Department of Electronic and Electrical Engineering, University of Strathclyde, Glasgow G1 1XW, United Kingdom*

Abstract

This paper develops two optimal control models for the energy management of a mining crushing process based on jaw crushers. The performance index for both models is defined as the energy cost to be minimized by accounting for the time-of-use electricity tariff. The first model is referred to as a variable load-based optimal control with the feeder speed and closed-side setting of the jaw crusher as control variables. The second model is the optimal switching control. From the simulation results, it is demonstrated that there is a potential of reducing the energy cost and energy consumption associated with the operation of jaw crushing stations in deep mines while meeting technical and operational constraints. Due to the inefficiency of the jaw crushing machine, whose no-load power consumption is between 40 and 50% of its rated power, the optimal switching control technique is shown to be a better candidate in reducing both energy cost and consumption of the jaw crushing station. The benefit of having an ore pass with a big storage capacity is shown to be of great importance in achieving more energy cost reduction of the primary jaw crushing station while improving the switching frequency profile associated with the switching controller.

Keywords: Energy management; optimal control; deep mines; Jaw crushing process; Time-of-use tariff.

1. Introduction

Due to the difficulty of the power utilities in continuously meeting the steadily growing energy demand, demand-side management (DSM) scheme is being implemented in several countries in the world. The aim of DSM is to plan the power grid at the customers' side in such a way to influence their energy consumption behaviour in order to meet the utility's desired load shape [1].

*Corresponding author. Tel.:+27 12 420-5789; fax: +27 12 362-5000.
Email address: papy.numbi@up.ac.za (B.P. Numbi)

In South Africa for instance, Eskom, the main electricity supplier, introduced the time-of-use (TOU) tariff-based DSM in the 1990s due to the electricity crisis, by trying to motivate customers to shift their loads out of the peak period [2].

Nomenclature	
$p(t)$	time-of-use electricity (TOU) tariff ($currency$)
W_i	bond's work index of ore ($kWh/short-ton$)
P_{80}	particle size that is larger than 80% by mass, of all particles in a product material sample (m)
F_{80}	particle size that is larger than 80% by mass, of all particles in a feed material sample (m)
Q_{OVS} and Q_{UDS}	respectively, mass flow rates of oversize and undersize run-of-mine (ROM) ore material (t/h)
CSS and T	closed-side setting and throw of the jaw crusher (m)
S_F	ore shape
F_{max}	maximum size of the feed ore material (m)
S_C	opening of the screen/distance between grizzly bars (m)
Q_F	mass flow rate of ROM ore material from the feeder to the scalper (t/h)
V	linear speed of the apron feeder (m/s)
ρ	bulk density of the ore material (t/m^3)
B	skirt width of the apron feeder (m)
D	bed depth of material on the apron feeder (m)
η_V	volumetric efficiency of the apron feeder
γ	undersize fraction or ratio of the ore material
$F_{80_{USC}}$	F_{80} for unscalped feed ore material (m)
η_D	overall drive efficiency
P_0	no-load mechanical power of the jaw crusher (kW)
t_S and j	sampling period ($hour$) and j^{th} sampling interval
N_S	total number of sampling intervals
p_j	electricity price at j^{th} sampling interval ($currency$)
"min" and "max"	minimum and maximum of the variable
P_{max}	maximum size of the ore product material (m)
P_{max}^{up}	upper bound/limit of P_{max} (m)
M_{ROM}	mass of ROM ore available in the storage system (t)
Q_{ROM}	mass flow rate of ROM ore material into the ore pass storage system (t/h)
$M_{ROM_{(0)}}$	initial value of M_{ROM} (t)
Q_{PR}	mass flow rate of ROM ore from the jaw crusher (t/h)
N	rotational speed of the jaw crusher (rpm)
w and G	width and gap of the jaw crusher (m)
D_V	vertical depth between jaws (m)
F_{av}	average feed size (m)
M_{TPR}	total mass production of the crushed ROM ore (t)
p_o, p_s, p_p	off-peak, standard and peak TOU electricity prices

Mining sectors account for about 15% of the total electrical energy consumption in South Africa, of which gold mining leads with 47% followed by platinum mining, taking 33% whilst 20% is consumed by the remaining mines[1]. It is further indicated that processing occupies the second place in mining energy consumption within the country with 19% of the total energy, preceded by materials handling which consumes 23%. This shows that mining sectors, especially gold mines have an important role to play in reducing South Africa's peak load, which will also reduce the cost associated with their energy consumption.

For materials handling in mining sectors, some research works have been carried out to investigate the potential of reducing the energy cost based on TOU tariff. In [3] for instance, the DSM technique is studied for an optimal hoist scheduling of a deep level mine twin rock winder system. Optimal energy control strategies for coal mining belt conveyors are investigated in [4, 5, 6, 7]. All of these studies demonstrate a great potential in reducing the energy cost associated with the operation of mining materials handling based on TOU tariff.

However, there have been relatively less research works dedicated to the energy cost management of comminution (crushing and grinding) circuits which are the first two stages of mineral processing in mining industries. A recent research paper was published in the area of energy cost optimization of a run-of-mine (ROM) ore grinding/milling circuit [8]. It is shown that a cost reduction of $9.90 per kg of unrefined product can be achieved when the optimal energy cost management is applied to a ROM ore grinding circuit processing platinum. Very few research works have been so far attempted in crushing electricity bill reduction. Other papers such as [9, 10, 11, 12, 13], use the TOU tariff-based DSM for the optimal operation of a water pumping station. An optimal load management for air conditioning loads is studied in [14], where a case study shows a reduction of 38% in peak demand with an annual cost saving of 5.9%, under TOU tariff. The benefit of the optimal load shifting based on TOU tariff, with application to manufacturing systems is also shown in [15]. In [16, 17], a dynamic or more flexible TOU tariff-based DSM, referred to as real time pricing-based DSM is applied to the optimal scheduling of electrical energy supply systems.

Compressive crushers such as jaw, gyratory and cone crushers are known to be inefficient machines with the no-load power ranging from 30 to 50% of their rated power [18, 19] . Hence, one way to improve the efficiency of these machines is through their operation efficiency by reducing their energy consumption and cost during their operation.

Jaw crushers, specially, form the core heavy-duty machines used since decades for crushing of coarse and hard ROM ores such as gold, Copper, Cobalt, Zinc ores, etc., in primary stations of mining industries [20, 21, 22]. These are also used for the same purpose for run-of-quarry (ROQ) rocks in aggregate industries.

[1]Eskom, The Energy Efficiency series: Towards an energy efficient mining sector, <http://www.eskomidm.co.za>

In the past, the common objectives in mining comminution process consisted of achieving a large production capacity (throughput maximization) and amount of fines [8]. Minimizing the energy consumption has been put as the last objective due to the relatively lower electricity price in the past. However, due to the electricity crisis encountered by many countries nowadays, the electricity price is seen to annually increase at a big rate. An annual price increase of 8% will be applied from 01-April 2013 to 31-March 2018 in South Africa for instance[2]. Hence, for a primary crushing circuit, the control objectives can be adapted as follows (adapted from [8]):

— achieve a product size less than a specified value,

— achieve a specified average production capacity (throughput) over a given period by minimizing the costs associated with the power consumption.

This paper is our first attempt to the optimal control for energy cost minimization in a primary crushing station of deep underground mines. Two techniques which take into account the TOU tariff are developed. One is referred to as the variable load (VL)-based optimal control while the other one is the optimal switching control. The former takes account of the jaw crushing energy model and optimally coordinates the feeder speed, closed-side setting and the working time of the jaw crusher for energy cost minimization. The optimal switching control optimally coordinates the on/off status and working time of the jaw crushing station to achieve the energy cost reduction; this is referred to as optimal load shifting. Solutions of the two techniques are compared to the current strategy used as a baseline solution in order to validate the effectiveness of the results.

This work is laid out as follows: Section 2 presents the mathematical formulation of the two optimal control techniques and the current control model of the primary jaw crushing station. The simulation results are given and discussed in section 3 before concluding the work in the last section.

2. Model development

2.1. System description

Figure 1 shows a typical configuration of a deed underground mine. The coarse ROM/blasted ore is loaded from different production stops (muckpiles) by Load-Haul-Dump (LHD) vehicles, and hauled to the tipping points [23] of the ore pass from where the ore material is transferred by gravity to the lower level of the mine. On the collection level, the ore is reduced to smaller size by primary crushers and stored in a storage buffer such as ore bin or silo. The crushed ore is then transported to the bottom of the shaft station by conveyor belts, dump trucks or trains (in this figure, a conveyor belt is considered), loaded into skips/buckets and hoisted to the surface bins, silos or stockpiles by the rock winder. From here, the ore is transported to the production plant for further

[2]Eskom, Revenue Application - Multi Year Price Determination 2013/14 to 2017/18 (MYPD3), <http://www.eskom.co.za>

processes such as secondary and tertiary crushing, grinding/milling, concentration, etc., for extraction of the valuable mineral.

Figure 1: Typical configuration of a deep underground mine (adapted from [24])

Figure 2: Primary jaw crushing station in a deep mine

The primary jaw crushing station is usually installed underground in mines and operates in open circuit as shown in Figure 2. The ROM ore is fed to the crushing station through the discharging zone, also called gate of the ore pass, at a controlled mass flow rate. This flow rate is usually controlled through a control gate at the ore pass exit zone by using control chains, a chute with control chains [23, 25, 26, 27] or an ore feeder [27]. Apron feeder and vibrating feeder are the main machines used to feed the ROM ore to primary crushers. In this work, an apron feeder is used for flow rate control.

The different components in this primary crushing station are:

– ore pass and feed hopper system: a storage buffer that receives the ore dumped from LHD vehicles;

– apron feeder: machine used to control the ore flow rate from the ore pass and feed hopper system;

– vibrating grizzly: a scalping equipment that receives the controlled ore flow rate from the apron feeder and feeds the jaw crusher by scalping (removing) fines (ROM ore size less than the closed-side setting of the jaw crusher);

– primary jaw crusher: a compressive crusher machine used for crushing of coarse and hard ROM ore;

– ore bin: a storage equipment to receive the crushed ore material that will be later conveyed to the shaft station.

2.2. General assumptions for the system

1. The time delay associated with the crushing process, from the ore pass tipping points to the ore bin is ignored;

2. The start-up and shut down energy consumptions of the jaw crusher are neglected;

3. The storage capacity of the ore bin is sufficient to store the total mass production of the ore material crushed for the given control horizon.

2.3. Model for VL-based optimal control of a primary jaw crushing process

The model involves the energy model of the jaw crushing process and achieves the system energy cost minimization through the coordination of the feeder speed, the closed-side setting of the jaw crusher and the working time of the crushing process based on TOU tariff.

The objective in this work is to minimize the total energy cost, J_C, of a jaw crushing process, subject to physical and operation constraints, and mostly,

the power utility constraint such as the TOU electricity tariff $p(t)$ during the control interval defined by the initial time, t_0, and final time, t_f. This optimal energy control problem can be formulated as:

$$min\, J_C = \int_{t_0}^{t_f} f_P\left(V\left(t\right), CSS\left(t\right)\right) p\left(t\right) dt, \tag{1}$$

subject to different constraints that will be later defined. In equation (1), f_P denotes the power function of the jaw crusher.

The aim is therefore to find an optimal control law that will transfer the ROM ore from the ore pass and hopper storage system to the ore bin through a crushing process, with minimum energy cost, during the given operation period from t_0 to t_f. Continuous-time optimal control problems are traditionally solved by Pontryagin's maximum principle [28]. However, the applicability of this principle assumes that the objective function and the associated constraint functions are continuously differentiable, which is referred to as the smooth condition. As can be seen, the discrete nature of the TOU electricity price function may lead the energy cost function, expressed by equation (1) to be continuous but not differentiable and hence nonsmooth. Moreover, it is noted that for complex problems such as the one addressed in this work, a numerical approach may be a preferred alternative.

2.3.1. Objective function

Up to date, the generally accepted and explicit expression to predict the specific net energy consumption of comminution machines during material size reduction is given by Bond's law as follows (in kWh/short-ton) [29, 30]:

$$W = 10W_i\left(\frac{10^{-3}}{\sqrt{P_{80}}} - \frac{10^{-3}}{\sqrt{F_{80}}}\right). \tag{2}$$

Equation (2) can be expressed in kWh/metric-ton by a multiplication of 1.1. Hence, the net crushing power consumption will be a simple product of the specific net energy consumption (in kWh/metric-ton) and the feed mass flow rate to the crusher Q_{OVS}, as given below:

$$P_{Net} = 11W_i\left(\frac{10^{-3}}{\sqrt{P_{80}}} - \frac{10^{-3}}{\sqrt{F_{80}}}\right) Q_{OVS}. \tag{3}$$

For jaw crusher application, the specific energy term in equation (3) can be controlled by the closed-side setting CSS of the jaw crusher [21, 31] while the feed mass flow rate Q_{OVS} can be controlled through the apron feeder speed V [32]. Hence, as previously discussed, two control variables are used for the optimal control of energy cost in this work; these are CSS and V which are adjustable in real-time. From [21, 31] and [32], the relationships between the terms in equation (3) and the two control variables are given, respectively, by equations (4) and (5), as follows (in m):

$$\begin{cases} P_{80} = 0.85\,(CSS + T)\,, \\ F_{80} = 0.8 S_F F_{max} + 0.2 S_C, \end{cases} \tag{4}$$

and

$$Q_F = kV, \tag{5}$$

where

$$k = 3600 \rho B D \eta_V. \tag{6}$$

All apron feeder parameters are referred to its discharging zone. k is assumed to be constant. However, this may vary with the apron feeder speed during the operation. As can be seen from Figure 2, recall that the feed mass flow rate Q_{OVS} going to the jaw crusher is related to the feed mass flow rate Q_F from the apron feeder through the ore undersize fraction, as follows [21]:

$$Q_{OVS} = (1 - \gamma)\, Q_F, \tag{7}$$

where

$$\gamma = \frac{P_{80}}{F_{80\,USC}} = \frac{0.85\,(CSS + T)}{0.8 S_F F_{max}}, \tag{8}$$

with $F_{80\,USC} = 0.8 S_F F_{max}$.

Substituting equations (5) and (8) in equation (7) yields:

$$Q_{OVS} = \left(1 - \frac{1.0625\,(CSS + T)}{S_F F_{max}}\right) kV. \tag{9}$$

Hence, the mass flow rate from the vibrating grizzly (scalper), referred to as undersize mass flow rate Q_{UDS} can be expressed as:

$$Q_{UDS} = \left(\frac{1.0625\,(CSS + T)}{S_F F_{max}}\right) kV. \tag{10}$$

In this work, it is assumed that the scalping screen S_C of the vibrating grizzly used is controllable in real-time. Hence, by setting S_C to CSS so that the fines or feed material with size lower than CSS can always be removed by the vibrating grizzly, equation (4) becomes:

$$\begin{cases} P_{80} = 0.85\,(CSS + T)\,, \\ F_{80} = 0.8 S_F F_{max} + 0.2 CSS. \end{cases} \tag{11}$$

The total power consumption of the jaw crusher can be now expressed in terms of the two control variables, V and CSS by the following function:

$$\begin{aligned} f_P\,(V, CSS) = \tfrac{11 W_i}{\eta_D} \quad & \left[\left(\tfrac{1.0846.10^{-3}}{\sqrt{(CS+T)}} - \tfrac{10^{-3}}{\sqrt{(0.8 S_F F_{max} + 0.2 CSS)}}\right) \times \right. \\ & \left. \left(1 - \tfrac{1.0625(CSS+T)}{S_F F_{max}}\right) kV + P_0\right]. \end{aligned} \tag{12}$$

The no-load mechanical power consumption P_0 of the jaw crusher [33] is assumed to be constant for a given jaw crusher speed. Hence, the objective function given by equation (1) can be discretized as follows:

$$min\, J_C = \frac{11W_i}{\eta_D} t_S \sum_{j=1}^{N_S} p_j \quad \left[\left(\frac{1.0846.10^{-3}}{\sqrt{(CSS_j+T)}} - \frac{10^{-3}}{\sqrt{(0.8S_F F_{max}+0.2CSS_j)}} \right) \times \left(1 - \frac{1.0625(CSS_j+T)}{S_F F_{max}} \right) kV_j + P_0 \right]. \tag{13}$$

2.3.2. Constraints

A. Control variable limits.

$$CSS^{min} \leq CSS_j \leq CSS^{max},\ (1 \leq j \leq N_S), \tag{14}$$

$$V^{min} \leq V_j \leq V^{max},\ (1 \leq j \leq N_S). \tag{15}$$

B. Limits on maximum size of ore product P_{max} . Based on various data provided by manufacturers of jaw crushers, the product maximum size P_{max} has been shown to be directly proportional to CSS with a proportional constant of 1.5, that is, $P_{max} = 1.5CSS$[3]. This constraint can therefore be written as:

$$1.5CSS_j \leq P_{max}^{up},\ (1 \leq j \leq N_S). \tag{16}$$

C. Limits on mass storage capacity . The dynamics of the mass stored in the ore pass and hopper system can be expressed in discrete-time domain by a first order difference equation as follows:

$$M_{ROM(j)} = M_{ROM(j-1)} + t_S \left(Q_{ROM(j-1)} - kV_{j-1} \right),\ (1 \leq j \leq N_S). \tag{17}$$

By recurrence manipulation, the mass stored in the storage system at j^{th} sampling interval can be expressed in terms of the initial mass $M_{ROM(0)}$ as follows:

$$M_{ROM(j)} = M_{ROM(0)} + t_S \sum_{i=1}^{j} \left(Q_{ROM(i)} - kV_i \right),\ (1 \leq j \leq N_S). \tag{18}$$

Hence, the mass storage constraints are given as:

$$M_{ROM}^{min} \leq M_{ROM(0)} + t_S \sum_{i=1}^{j} \left(Q_{ROM(i)} - kV_i \right) \leq M_{ROM}^{max},\ (1 \leq j \leq N_S). \tag{19}$$

[3]Metso, C Series jaw crushers, <http://www.metso.com>

D. Limits on mass flow rate from the apron feeder.

$$Q_F^{min} \leq kV_j \leq Q_F^{max}, \ \ (1 \leq j \leq N_S)\,. \tag{20}$$

E. Mass balance in the jaw crusher. This equality constraint prevents the machine crushing chamber from obstruction [20]. The equation is given as follows:

$$Q_{OVS(j)} = Q_{PR(j)}, \ \ (1 \leq j \leq N_S)\,. \tag{21}$$

The analytical model of the product mass flow rate from the jaw crusher in terms of CSS is expressed as [31]:

$$Q_{PR} = 60Nw\,(CSS + 0.5T)\left(\frac{D_V T}{G - (CSS + T)}\right) K_1 K_2 K_3 \rho, \tag{22}$$

where $K_1 = 0.85 - \left(\frac{F_{av}}{G}\right)^{2.5}$, $K_2 = 1.92.10^{\frac{6.5T}{G}}$ and K_3 is assumed to be 0.6 for softer materials such as coal and 1 for harder materials.

For simplicity, equation (22) can be approximated to a linear function of CSS, taking advantage of the fact that the sum $(CSS + T)$ is generally too small compared to G. This therefore leads to a simpler equation:

$$Q_{PR} = 60K_4 NwCSS + 30K_4 NwT, \tag{23}$$

where $K_4 = \frac{D_V T K_1 K_2 K_3 \rho}{G}$.

For a given operational speed and material characteristics such as gradation, bulk density, crushability, moisture and clay content, jaw crusher manufacturers usually provide practical data expressing the relationship between Q_{PR} and CSS. Based on an ore density of $2.7t/m^3$ with a scalped feed, the curve fitting of the data for C-series jaw crushers[4] as shown by Figure 3 proves a linear relationship of the form:

$$Q_{PR} = aCSS + b. \tag{24}$$

Figure 3: Fit of throughput rate (in metric-ton/h) of C-series jaw crushers

In Figure 3, the markers indicate the real data and the solid lines represent their corresponding curve fitting. It can be seen that equation (24) validates the assumption of neglecting the sum $(CSS + T)$ before G since equations (23) and (24) are the same by identification of $a = 60K_4 Nw$ and $b = 30K_4 NwT$. The coefficients a and b can therefore be found either based on analytical model or manufacturer's data. The equality constraint given by equation (21) is finally expressed as:

$$\left(1 - \frac{1.0625\,(CSS_j + T)}{S_F F_{max}}\right) kV_j = aCSS_j + b, \ \ (1 \leq j \leq N_S)\,. \tag{25}$$

[4]Metso, C Series jaw crushers, <http://www.metso.com>

F. Limits on mass flow rate from the jaw crusher .

$$Q_{PR}^{min} \leq aCSS_j + b \leq Q_{PR}^{max},\ \ (1 \leq j \leq N_S)\,. \tag{26}$$

G. Total production requirement.

$$\sum_{j=1}^{N_S} \left(Q_{UDS(j)} + Q_{PR(j)}\right) t_S \geq M_{TPR}. \tag{27}$$

This can be rewritten as:

$$\sum_{j=1}^{N_S} \left(\frac{1.0625\,(CSS_j + T)}{S_F F_{max}} kV_j + aCSS_j + b \right) t_S \geq M_{TPR}. \tag{28}$$

2.3.3. Reduction of the problem dimension

The equality constraint given by equation (25) indicates the interdependency between the two control variables, namely the closed-side setting CSS of the jaw crusher and the apron speed V. In order to reduce the dimension of the problem and consequently, the computational time, CSS can be expressed from equation (25) in terms of V as follows:

$$CSS = \frac{kV\,(S_F F_{max} - 1.0625T) - bS_F F_{max}}{1.0625kV + aS_F F_{max}}. \tag{29}$$

Hence, equation (29) is substituted in the objective function as well as in all constraints to eliminate CSS in such a way to have the apron feeder speed V as the only control variable. This therefore reduces the problem dimension by half, from $2N_S$ to N_S. Furthermore, after some mathematical simplification, the optimization model can be finally expressed as:

$$\begin{aligned} min\, J_C\,(V_j) = \tfrac{11W_i}{\eta_D} t_S \textstyle\sum_{j=1}^{N_S} p_j \quad & \left[\left(\frac{1.0846.10^{-3}}{\sqrt{\left(\frac{kV_jC - bS_FF_{max}}{1.0625kV_j + aS_FF_{max}} + T\right)}} \right.\right. \\ & \left.\left. - \frac{10^{-3}}{\sqrt{\left(0.8S_FF_{max} + 0.2\frac{kV_jC - bS_FF_{max}}{1.0625kV_j + aS_FF_{max}}\right)}} \right) \right. \\ & \left. \times \left(a\frac{kV_jC - bS_FF_{max}}{1.0625kV_j + aS_FF_{max}} + b \right) + P_0 \right], \end{aligned} \tag{30}$$

where $C = S_F F_{max} - 1.0625T$, subject to

$$M_{ROM}^{min} \leq M_{ROM(0)} + t_S \sum_{i=1}^{j} \left(Q_{ROM(i)} - kV_i\right) \leq M_{ROM}^{max},\ (1 \leq j \leq N_S)\,, \tag{31}$$

$$kt_S \sum_{j=1}^{N_S} V_j \geq M_{TPR}, \tag{32}$$

$$
\begin{aligned}
&max\left(V_1^{min}, V^{min}, \frac{Q_F^{min}}{k}, V_3^{min}\right) \leq V_j \\
&\leq min\left(V_1^{max}, V^{max}, \frac{Q_F^{max}}{k}, V_2^{max}, V_3^{max}\right), (1 \leq j \leq N_S),
\end{aligned} \tag{33}
$$

where

$V_1^{min} = \frac{bS_F F_{max} + aS_F F_{max} CSS^{min}}{k(S_F F_{max} - 1.0625T) - 1.0625kCSS^{min}}$,
$V_1^{max} = \frac{bS_F F_{max} + aS_F F_{max} CSS^{max}}{k(S_F F_{max} - 1.0625T) - 1.0625kCSS^{max}}$,
$V_2^{max} = \frac{bS_F F_{max} + aS_F F_{max} P_{max}^{up}}{1.5k(S_F F_{max} - 1.0625T) - 1.0625kP_{max}^{up}}$,
$V_3^{min} = \frac{aS_F F_{max} Q_{PR}^{min}}{ak(S_F F_{max} - 1.0625T) + 1.0625kb - 1.0625kQ_{PR}^{min}}$ and
$V_3^{max} = \frac{aS_F F_{max} Q_{PR}^{max}}{ak(S_F F_{max} - 1.0625T) + 1.0625kb - 1.0625kQ_{PR}^{max}}$.

2.4. Model for optimal switching control of a primary jaw crushing process

Unlike in the previous case, this model does not involve the energy model of the jaw crusher. The controller optimally coordinates the on/off status and working time (based on TOU tariff) of the jaw crushing process in order to minimize the associated energy cost. Hence, for this case, the energy cost is reduced through load shifting based on TOU electricity tariff.

Due to the high no-load power of the jaw crusher, ranging from 40 to 50% of its rated power [18, 19], the switching frequency of this machine has to be minimized as much as possible in order to reduce the impact of mechanical stresses and high starting currents on the electric motor. The time delay is another concern when switching off the jaw crusher. The feeding equipment has to be stopped few minutes before switching off the jaw crusher. This precaution allows the crusher to have sufficient time to process all the ore material present in the crushing chamber, so as to avoid too large load for its next starting up.

To reduce the negative effect of the on/off switching frequency on the crusher drive system (electrical motor and drive transmission) as well as on the power supply systems, a soft stater is assumed to be available to the jaw crusher. In contrast to the VL-based optimal control model, here, the sampling time will be chosen to be large enough in such a way to further minimize the drawback of the multiple switching associated with the switching controller. The consideration of a larger sampling time will also allow us to neglect the time delay between switching off the feeder and jaw crusher, that can range from 1 to 3 minutes, depending on the size of the machine and working conditions. For these reasons, in the process system defined in Figure 2, the feeding equipment and jaw crusher can share the same switching function. This means that they are considered to be synchronously switched on or off when the relevant time delay is ignored.

2.4.1. Objective function

Here, the problem consists of optimally coordinating the on/off status of the jaw crusher in a synchronous way with that of the feeding equipment, in such a way to minimize the crushing energy cost based on TOU tariff. This is formulated as follows:

$$min\, J_C = \frac{1}{\eta_D} \sum_{j=1}^{N_S} \left(P_{Net-P_{max}^{up}} + P_0 \right) u_j p_j t_S = \frac{1}{\eta_D} P_t t_S \sum_{j=1}^{N_S} p_j u_j, \tag{34}$$

where $P_t = P_{Net-P_{max}^{up}} + P_0$ is the total crushing power consumption of the jaw crusher. In equation (34), $P_{Net-P_{max}^{up}}$ denotes the net crushing power consumption of the jaw crusher which corresponds to the upper bound of the maximum product size P_{max}^{up}. The closed-side setting CSS is therefore set in such away to satisfy the required P_{max}^{up}. The throughput flow rate of the jaw crusher is accordingly obtained. In equation (34), u_j is a discrete-switching function that takes the value of either 0 or 1. u_j means that the machines are switched on during the j^{th} sampling interval, while $u_j = 0$ denotes that the machines are switched off. The other notations are the same as in the previous problem.

2.4.2. Constraints

These are the limits on the mass storage capacity and also the requirement on the total mass production of ore.

A. Mass storage capacity .

$$M_{ROM}^{min} \leq M_{ROM(0)} + t_S \sum_{i=1}^{j} \left(Q_{ROM(i)} - Q_F u_i \right) \leq M_{ROM}^{max},\ (1 \leq j \leq N_S)\,. \tag{35}$$

B. Requirement on total production.

$$t_S \sum_{j=1}^{N_S} Q_F u_j \geq M_{TPR}. \tag{36}$$

Note that the mass balance $Q_F = Q_{OVS} + Q_{UDS}$ is supposed to be verified within the control interval.

2.5. Model for current control of a primary jaw crushing process

In practice, jaw crushers operate continuously in mining and aggregate industries. The feed rate is usually controlled in such a way to avoid the jaw crusher to be overloaded while achieving the plant production target. Hence, the current control model is formulated in the same way as VL-based optimal model defined in subsection 2.3, with the only difference being that the total production target is considered as the control objective to be achieved. This is formulated as minimizing the quadratic deviation function, J_{PR}, between the actual plant production and the total plant production target M_{TPR}.

$$min\, J_{PR} = \left(k t_S \sum_{j=1}^{N_S} V_j - M_{TPR} \right)^2, \tag{37}$$

subject to constraints (31)-(33).

3. Simulation results

3.1. Algorithms

Several optimization algorithms can be used to solve the problems defined in this work.

Since the VL-based optimal control problem has a nonlinear objective function, based on convexity assumption, the $fmincon$ function of MATLAB R2013 Optimization Toolbox is used. Its canonical form is given as follows:

$$min\, f\left(X\right) \tag{38}$$

subject to

$$\begin{cases} AX \leq b\ \left(linear\, inequality\, constraint\right), \\ A_{eq}X = b_{eq}\ \left(linear\, equality\, constraint\right), \\ C\left(X\right) \leq 0\ \left(nonlinear\, inequality\, constraint\right), \\ C_{eq}\left(X\right) = 0\ \left(nonlinear\, equality\, constraint\right), \\ L_b \leq X \leq U_b\ \left(lower\, and\, upper\, bounds\right). \end{cases} \tag{39}$$

For VL-based optimal control, the vector X contains the feeder speed for all sampling intervals. Three linear inequality constraints of which two of (31) and one of (32) are integrated into A and b. The lower and upper boundary constraints (33) are in incorporated into L_b and U_b. After solving the problem, recall that the correponding CSS control variables at each sampling interval are obtained using equation (29).

The optimal switching control is solved using the ga function of MATLAB R2013 Optimization Toolbox that can easily handle mixed-inter, integer or binary optimization problems with lower computational time[5]. The canonical form of ga is the same as for the $fmincon$ function, except that for this problem, the control variable is the on/off status of the jaw crushing station, denoted by u_j which is set to be an integer number bounded within [0, 1].

The objective function of the current control model is a nonlinear function. Hence, the $fmincon$ function of MATLAB 2013 Optimization Toolbox is also used for the current control model.

3.2. Data presentation

3.2.1. Time-of-use electricity tariff

One of the important parameters in the optimal energy control problem formulated in this work is the time-of-use (TOU) electricity tariff. The recent Eskom Megaflex Active Energy-TOU tariff (non-local authority rates) with VAT included is used for a high-demand season weekday in this case study. The high demand season (from June to August) is chosen since the peak period is charged at a very high cost compared to the lower demand season. The energy cost

[5]Matlab, Mixed Integer Optimization, <http://www.mathworks.com>

management for the high demand season is therefore crucial for electricity bill reduction. However, a slight modification is made to this TOU tariff in order to better appreciate the effectiveness of the model. The time interval of the standard period, [20, 22] is considered to be a peak period. This is given as[6]:

$$p(t) = \begin{cases} p_o = 0.3656R/KWh \; if \; t\epsilon [0,6] \cup [22,24], \\ p_s = 0.6733R/KWh \; if \; t\epsilon [6,7] \cup [10,18], \\ p_p = 2.2225R/KWh \; if \; t\epsilon [7,10] \cup [18,22], \end{cases} \tag{40}$$

where R is the South African currency Rand and t is the time of any weekday in hours (from 0 to 24).

The control horizon $[t_0, t_f]$ and sampling time t_S of, respectively, 24h and 10 min are used for VL-based optimal control and current control problems. As discussed in subsection 2.4, a relatively large sampling time of 30 min, not greater than the shortest time period of the change in TOU tariff function $p(t)$ is used for the optimal switching control in order to reduce the machine switching frequency. This means that the time period between two consecutive start-ups of the jaw crusher cannot be less than 30 minutes.

3.2.2. Ore pass storage system and ore characteristics

Note that the hopper capacity may be neglected compared to that of the ore pass. In this study, the ore pass capacity of one of South African deep mines processing gold is considered [34]. For this ore pass, the diameter is 2.4m and the length or height is 170m. To ensure free flow, it is reported that the ratio between the ore pass dimension diameter D_{OP} and the largest ROM ore size F_{max} lies between 3 and 10 [23]. Hence, with a minimum ratio of 3, the maximum ore size of ore gold is assumed to be 0.8m for this case study. With the ore bulk density of gold ore being $2.7t/m^3$,[7] the maximum storage capacity of the ore pass is calculated as $170 \times 2.7 \times \pi (2.4)^2 /4 = 2075t$. The minimum storage capacity is set to 10% of the maximum capacity. The ore shape factor S_F of 1.7 (cubic ore shape) is considered, while the average Bond's work index W_i of gold ore is $14.83KWh/short-ton$ [21].

3.2.3. Jaw crusher, apron feeder and vibrating grizzly

For simulation purpose, a primary jaw crushing station is assumed to be installed under the ore pass above described.

In general, the largest feed size (lump size) is the major index for the choice of processing equipments such as crushers, feeders and scalpers; the flow rate capacity follows.

[6] Eskom, Tariffs & Charges Booklet 2013/2014, <http://www.eskom.co.za>

[7] Ari Jaakonmaki and Metso, Aspects of Underground Primary Crusher Plant Design,<http://www.miningcongress.com>

A. Jaw crusher . For a jaw crusher, the maximal feed size F_{max} should be equal or less than 85% of its gap G, that is, $F_{max} \leq 0.85G$ [21]. Hence, with $F_{max} = 800mm$, G should be larger than 940mm. With this, C160 jaw crusher is used. Technical data and other specifications of C160 are as follows[8]: $G = 1200mm$, the installed power is 250kW, $CSS^{max} = 300mm$, $CSS^{min} = 150mm$, extended to 100mm for simulation purpose (since smaller CSS is practically possible with a machine reduction ratio that can go up to 10/1 [18]). The throw T is obtained to be 0.06m (60mm) based on the formula, $T = 0.0502G^{0.85}$ [21]. The crusher speed N is $220rpm$, the no-load power P_0 of the jaw crusher is assumed to be 40% of its rated power, that is, 100kW for C160 jaw crusher. The fitting coefficients of the C160 throughput capacity found from Figure 3 are: $a = 2543$ and $b = 50$. Hence, the maximum and minimum flow rates of the C160 jaw crusher are found to be respectively, $813t/h$ and $304t/h$. The overall drive efficiency η_D is assumed to be 0.95.

B. Apron feeder . An apron feeder with a skirt width B bigger than 1600mm is considered (since $B \geq 2F_{max}$). This corresponds to the apron feeder span width of 1829mm[9]. With a clearance of 100mm between the pan width and skirt, B is found to be 1729mm for this apron feeder. The bed depth D is obtained as $0.75B = 1297mm$. The maximum speed of the feeder is $60fpm = 0.3048m/s$ which corresponds to $Q_F^{max} = 5000t/h$, with $\eta_V = 0.75$ when using equation (5).

3.2.4. Vibrating grizzly or Scalper

The vibrating grizzly is used for scalping (removing) fines from the ROM ore without controlling the flow rate. This machine is therefore considered as a simple separation point with appropriate stroke length, speed, and inclination angle for scalping efficiency.

3.2.5. Ore bin and ore production requirement

The capacity of the ore bin is assumed enough to store the total plant production target M_{TPR} for 24h. The maximum of ore production is to be achieved by meeting equipment constraints and product quality. The product quality is expressed in terms of the maximum size of product material P_{max} given by equation (16), which should be equal or less than 400mm (0.4m).

3.3. Results and discussion

Usually, an ore pass has several tipping points where a mass flow rate Q_{ROM} is dumped into it by LHD vehicles from different stops. The intermittent characteristic of LHD feeding devices makes Q_{ROM} to be uncontrollable but predictable. For all simulation cases, the forecast of the feed rate Q_{ROM} is assumed to vary around $700t/h$ as given bellow:

[8]Metso, C Series jaw crushers, <http://www.metso.com>
[9]Metso, World-Class Apron Feeders, <http://www.metso.com>

$$Q_{ROM}(t) = \begin{cases} 680t/h \; if \; t\epsilon\,[0,6]\,, \\ 720t/h \; if \; t\epsilon\,[6,12]\,, \\ 700t/h \; if \; t\epsilon\,[12,18]\,, \\ 690t/h \; if \; t\epsilon\,[18,24]\,, \end{cases} \tag{41}$$

where t is the time of an weekday in hours (from 0 to 24). For all simulation scenarios in this work, the initial ore mass in the ore pass storage system $M_{ROM(0)}$ is assumed to be 50% of the maximum ore pass capacity M_{ROM}^{max}, while the total plant production target M_{TPR} is fixed to 15000t for 24 hours.

3.3.1. Performance analysis of the optimal control techniques

Case I: Ore pass with maximum storage capacity of 2017t. Figures 4 and 5 show the simulation results for the current control and VL-based optimal control strategies. The legends of Figure 4 also apply to Figure 5. The result for optimal switching control is shown in Figure 6. Tables 1-3 gives the performance of the optimal control techniques used. For the optimal switching control technique, a closed-side setting CSS of 0.266m that limits the maximum product size from the C160 jaw crusher to 0.4m is used. The corresponding throughput rate and net crushing power consumption are found, respectively, to be $726.4t/h$ and $114.67kW$. The undersize fraction is therefore found to be 0.2536, which based on mass balance, yields a mass flow rate from apron feeder Q_F of $973.2t/h$, feeder speed V_F of $0.06m/s$, and undersize feed rate Q_{UDS} of $246.8t/h$. Note that the dotted lines in Figures showing the simulation results, denote the maximum and minimum of the variable.

The feasibility of both optimal control approaches is shown through Figures 4-6. As can be seen from Figures 4 and 5, with the current control strategy, the crushing plant continuously runs without consideration of the TOU tariff. It is easy to notice that the feeder speed V_F, feeder flow rate Q_F and the crusher flow rate Q_{PR} are almost evenly distributed for a long period within the control interval. This will result in high energy cost as the peak-load is not reduced or shifted since the TOU tariff is not taken into account in the control scheme. However, the VL-based optimal controller shifts as much the crusher load Q_{PR} as possible, out of peak period by optimally decreasing the feeder speed V_F and hence the feeder flow rate Q_F and the jaw crusher flow rate Q_{PR} during peak periods in order to minimize the crushing energy cost. The feeder speed is increased for a long period, during off-peak and standard periods in order to meet the total production target of the station as given in Table 1, at a cheaper energy cost. During these periods, the closed-side setting CSS of the jaw crusher will continuously follow the pattern of V_F as shown from the first graphs of Figure 4 and Figure 5, in order to meet all the time, the mass balance constraint of the jaw crusher (input flow rate Q_{OVS} = output flow rate Q_{PR}). This also demonstrates that the relationship between the closed-side setting CSS of the jaw crusher and the apron feeder speed V, given by equation (29) is almost linear, which will lead the mass flow rates Q_F, Q_{PR}, Q_{OVS}, Q_{UDS} to also have a linear relationship with either of the two control variables (V and

CSS) as can be seen from Figures 4 and 5. For this reason, achieving a relatively high energy cost reduction with VL-based optimal controller is limited due to the fact that the decrease of V_F and hence Q_F and Q_{PR} will be restricted by the constraints imposed on CSS of jaw crusher. As given in Tables 2 and 3, 6.09 % of cost saving and 2.54 % of energy saving are achieved. It is therefore worthy to mention that more than half of the energy cost reduction is due to the optimal shifting of the crusher load based on TOU tariff whilst the rest comes from the 2.54% of energy saving.

With respect to the mass storage dynamics given by the second graph of Figure 4, the same conclusion as previously discussed can be drawn. It is shown that, unlike the current control strategy, during peak period, the ore mass M_{ROM} is greatly stored (increased) instead of being fed to the crusher, while in off-peak and standard periods, a large amount of ore material is drawn from the ore pass storage system and fed to the crusher due to the lower energy cost. The effectiveness of the algorithm is also demonstrated with regards to the constraints. Figures 4 and 5 show that all control and dependent variable constraints lie within their limits. Although the predicted maximum product size from the jaw crusher is not plotted, the first graph of Figure 5 indicates that the closed-side setting CSS of the jaw crusher will never go beyond 0.2661m, which corresponds to a maximum of ore product size of 0.399m, less than 0.4m (fixed as requirement).

For optimal switching control strategy, it is inferred from Figure 6 that during peak period, the jaw crushing station is on off-status for a longer period than when it is on on-status so that the ore mass M_{ROM} is stored as much as possible. However, this is not the case for off-peak and standard periods where the on-status period is rather longer than off-status period due to the lower energy cost and also to meet the 24h production capacity. From Tables 2 and 3, a cost saving of 45.92% and energy saving of 30.12% are achieved with the optimal switching control of the jaw crushing station.

In contrast to findings in [4] for optimal energy control of belt conveyors, it is shown in this work, that the optimal switching control strategy yields more cost saving and energy saving than the VL-based optimal control strategy. However, this is achieved at the cost of switching the machines. Note that the VL-based optimal control in [4] is referred to as variable speed drive (VSD)-based optimal control. Two reasons could explain the higher savings achieved by the optimal switching control approach. The first and major reason is that compressive crushers such as jaw crushers are inefficient machines due to their no-load power consumption ranging between 40 to 50% of the total power consumption. This means that running continuously, the jaw crusher will lead to almost 50% of energy consumption which does not contribute to the work done and therefore regarded as a waste of energy and money. Hence, by optimally switching the jaw crushing station, both net crushing and no-load power consumptions are shifted, while with VL-based optimal control approach, only the net crushing power consumption can be controlled. The second reason is that the net crushing power of the jaw crusher is not controllable to zero with VL-based optimal control. This is due to the lower constraint imposed on CSS, preventing the

crusher throughput rate Q_{PR} from being controlled to zero during peak period (see Figure 5), in order to achieve more energy cost reduction.

Figure 4: VL-based optimal control and current control techniques-case I

Figure 5: VL-based optimal control and current control techniques-case I (continued)

Figure 6: Optimal switching control technique-case I

Case II: Ore pass with maximum storage capacity doubled to 4150t. In order to analyse the influence of the size of the ore pass storage system on the performance achieved by the two optimal energy control strategies, the previous storage capacity considered in case I, is doubled. Figures 7-9 show the results for this case study. As discussed in case I, it is also seen that the energy cost is reduced with VL-based optimal control strategy as compared to the current control strategy. This is due to the fact the load is shifted as much as possible out of the peak period when using VL-based optimal control, while with the current control technique, the load is kept almost constant along the control interval. However, with the same initial condition (the initial mass stored in the ore pass is half of its maximum storage capacity) and production requirement (greater or equal to 15000t), it is obvious that the increase in storage capacity leads to a higher initial amount of ore material as compared to case I. This means that with case II, at the beginning of the control interval, a larger amount of ore material will be available and therefore processed during off-peak period, leading to a smaller amount of ore material to be processed during standard period. This can be seen by comparing Figures 4-5 of case I with Figures 7-8 of case II, where it is shown that with case I, the apron feeder and jaw crusher operate for a shorter period at, respectively, higher speed V_F, feeder flow rate Q_F, and crusher flow rate Q_{PR} during off-peak period (from 0 to 6h) due to the lower initial stored material, as compared to case II. Hence, in order to meet the production requirement, the same figures show that during standard period, with case I, the apron feeder and jaw crusher operate for a longer period at higher load (Q_F and Q_{PR}), with comparison to case II.

Since with case II, a larger amount of ore material is shifted from standard and peak periods to off-peak period when compared to case I, one would expect more cost saving to be achieved with case II. However, Table 1 shows that the energy cost and energy consumption in case II are almost equal to those obtained in case I. This is due to the fact that, with VL-based optimal control in case II, a slight larger amount of load is processed during [18, 22h] peak period, at a very high energy cost, in order to meet the production requirement. One of the reasons why the increase in storage capacity does not improve the energy and cost savings is the fact that the optimization search space is very restricted by the constraints imposed on CSS, as previously explained.

From Tables 2 and 3, it is noticed that the increase in storage capacity leads to a slight decrease of cost saving, by 1.3377% (from 6.0893 to 4.7516%) and energy saving, by 0.1655% (from 2.5375 to 2.3720%) as compared to case I. This is explained by the lower production capacity achieved with case II (15004t) as compared to case I (15703t), while both energy cost and energy consumption for the two cases are almost the same as previously mentioned.

With the optimal switching control strategy, Figure 9 shows that the increase of ore pass storage capacity will have a positive impact in reducing the switching number of the jaw crushing station. In case I, the jaw crushing station is switched on, eight (8) times, while in case II, the station is switched on, four (4) times only. As compared to Figure 6 of case I, Figure 9 of case II shows that almost all peak-load is shifted out from peak-time period, which therefore explains the increase of the energy cost saving from 45.92% to 64.9% as shown in Table 2. However, from Table 3, it is shown that, increasing the ore pass capacity does not yield a significant improvement in energy saving as compared to case I.

3.3.2. Corollary

The simulation results show that due to the high no-load power consumption of the jaw crusher, the optimal switching control of the jaw crushing process can achieve considerable energy saving and cost saving as compared to the variable load-based optimal control.

However, switching the jaw crusher will result in severe impact in practice. During the starting period, the high no-load power consumption of the jaw crusher will be responsible of high current transients or starting current and torque pulsations on the jaw crusher itself, the drive electrical motor, electrical power supply system and even the concrete foundation supporting the crusher.

On one hand, a high starting current will lead to the electrical stress on the electrical motor winding and power system components such as transformers, electrical cables, transmission lines, generators, breakers, etc. On the other hand, high starting torque pulsations will lead to mechanical stress on mechanical drive systems such as the drive belt, bearings and shafts of the motor and crusher. Moreover, the vibrations caused by the high amplitude of the pulse of the starting motor torque will be transmitted to the concrete foundation of the crusher and lead to the pavement vibration and noise. This will therefore justify a negative impact on the practical working environment.

Nowadays, a soft starter is being used to solve the aforesaid problem [35]. Another option is to use a variable speed drive (VSD). The use of a soft starter or VSD device makes it possible to smooth the motor acceleration caused by the high transient accelerating torque, while reducing the starting current of the electrical motor at the same time. The reduction of the pulse magnitude of the motor torque will also decrease the vibration and noise level in the working environment. Hence, some of the benefits from reducing the mechanical stress will be the improvement of the lifespan and reliability of the mechanical drive components, as well as the concrete foundation of the crusher.

Smoothing the accelerating torque will result in reduction of the starting current, which will lead to minimization of the electrical stress on both electrical motor winding and power system components. Some of the benefits from this are the energy efficiency improvement, since less line current is drawn from the power supply systems. It will also allow several crusher motors to be started more frequently for their optimal energy management, therefore allowing the overall load management within a cluster approach.

In practice, if the jaw crusher is not equipped with a soft starter or VSD device, an extra capital cost needs to be considered. However, for a constant speed application such as jaw crushing process, the soft starter can be seen competitive in terms of cost and efficiency as compared to VSD. Furthermore, a very short payback period can be expected due to the larger energy and cost savings achieved by optimal load shifting, but also the cheaper initial capital cost of the soft starter.

Figure 7: VL-based optimal control and current control techniques-case II

Figure 8: VL-based optimal control and current control techniques-case II (continued)

Figure 9: Optimal switching control technique-case II

Table 1: Total ore production and corresponding energy cost and consumption

Techniques	Total ore production (t)	Energy cost (R)	Energy consumption (kWh)
CASE I: $M_{ROM}^{max} = 2075t$			
Current control	15703	5368.1	5217.9
VL-based optimal control	15703	5041.2	5085.5
Optimal switching control	16058	2968.4	3728.5
CASE II: $M_{ROM}^{max} = 4150t$			
Current control	15000	5304.6	5194.0
VL-based optimal control	15004	5053.9	5072.2
Optimal switching control	15085	1871.5	3502.5

Table 2: Cost savings of the optimal control techniques

Techniques	Unit energy cost (R/t)	Cost saving (%)
CASE I: $M_{ROM}^{max} = 2075t$		
Current control	0.3419	/
VL-based optimal control	0.3210	6.0893
Optimal switching control	0.1849	45.927
CASE II: $M_{ROM}^{max} = 4150t$		
Current control	0.3536	/
VL-based optimal control	0.3368	4.7516
Optimal switching control	0.1241	64.916

Table 3: Energy savings of the optimal control techniques

Techniques	Unit energy consumption (kWh/t)	Energy saving (%)
CASE I: $M_{ROM}^{max} = 2075t$		
Current control	0.3323	/
VL-based optimal control	0.3239	2.5375
Optimal switching control	0.2322	30.125
CASE II: $M_{ROM}^{max} = 4150t$		
Current control	0.3463	/
VL-based optimal control	0.3381	2.3720
Optimal switching control	0.2322	32.945

4. Conclusion

The inefficiency of compressive crushers such as jaw crusher may lead to considerable energy consumption and cost during their operation. Hence, one way to solve this problem is to improve the efficiency of these machines during their operation.

This paper develops two optimal control techniques for the TOU based-optimal energy management of a jaw crushing station in deep mines under both physical and operating constraints. The first technique is referred to as a variable load (VL)-based optimal control, while the second one is an optimal switching control. The proposed techniques are useful to fill the gaps in the literature towards the energy efficiency improvement in crushing processes, which will also result in carbon emission reduction.

Two scenarios are carefully studied in order to analyse the influence of the storage capacity on the developed models. With the initial storage capacity, it is shown that 6.09% and 2.54% of cost and energy savings are, respectively, obtained when VL-based optimal control strategy is used. With the optimal switching control technique, 45.92% of cost saving and 30.12% of energy saving are achieved. When the initial storage capacity is doubled, the VL-based optimal

control does not show any improvement on both cost and energy consumption, while with the optimal switching control strategy, an energy cost saving of 64.9% is achieved as compared to 45.92% in the initial case (case I).

Hence, through the simulation results, it is shown that, unlike the VL-based optimal controller, the optimal switching controller has a greater potential to achieve high reduction of both energy consumption and cost of a jaw crushing process. However, this is achieved at the cost of switching the machines. With the same ore production requirement, the influence of using a larger storage capacity is seen to be of considerable benefit in reducing the switching number of the process and further achieving more energy cost saving. Moreover, it is suggested that a soft starter be used in order to reduce the negative impact of the on/off switching of the jaw crusher when using the optimal switching control technique.

5. References

References

[1] Gellings C. The concept of demand-side management for electric utilities. Proceedings of the IEEE 1985;73(10):1468–70.

[2] Ramsbottom D. Case study into the application of time of use tariffs in the Eskom Western Region of South Africa in reducing peak loads. in: Cigré 2009 6th South African Regional Conference: Somerset West; Western Cape, South Africa; 17–21 August, 2009.

[3] Badenhorst W, Zhang J, Xia X. Optimal hoist scheduling of a deep level mine twin rock winder system for demand side management. Electric Power Systems Research 2011;81(5):1088–95.

[4] Zhang S, Xia X. Optimal control of operation efficiency of belt conveyor systems. Applied Energy 2010;87(6):1929–37.

[5] Zhang S, Xia X. Modeling and energy efficiency optimization of belt conveyors. Applied Energy 2011;88(9): 3061–71.

[6] Mathaba T, Xia X, Zhang J. Optimal scheduling of conveyor belt systems under critical peak pricing. in: 10th International Power and Energy Conference, IPEC 2012; Ho Chi Minh, Vietnam; 12–14 December, 2012.

[7] Middelberg A, Zhang J, Xia X. An optimal control model for load shifting - With application in the energy management of a colliery. Applied Energy 2009;86:1266–73.

[8] Matthews B, Craig I. Demand side management of a run-of-mine ore milling circuit. Control Engineering Practice 2013;21(6):759–68.

[9] Zhang H, Xia X, Zhang J. Optimal sizing and operation of pumping systems to achieve energy efficiency and load shifting. Electric Power Systems Research 2012;86:41–50.

[10] Zhuan X, Xia X. Optimal operation scheduling of a pumping station with multiple pumps. Applied Energy 2013;104:250–7.

[11] Van Staden AJ, Zhang J, Xia X. A model predictive control strategy for load shifting in a water pumping scheme with maximum demand charges. Applied Energy 2011;88(12):4785–94.

[12] Zhuan X, Xia X. Development of efficient model predictive control strategy for cost-optimal operation of a water pumping station. IEEE Transactions on Control Systems Technology 2013;21(4):1449–54.

[13] Pelzer R, Mathews E, Le Roux D, Kleingeld M. A new approach to ensure successful implementation of sustainable demand side management (DSM) in South African mines. Energy 2008;33(8):1254–63.

[14] Ashok S, Banerjee R. Optimal cool storage capacity for load management. Energy 2003;28(2):115–26.

[15] Wang Y, Li L. Time-of-use based electricity demand response for sustainable manufacturing systems. Energy 2013;63:233–44.

[16] Mitra S, Sun L, Grossmann IE. Optimal scheduling of industrial combined heat and power plants under time-sensitive electricity prices. Energy 2013;54:194–211.

[17] Faria P, Vale Z. Demand response in electrical energy supply: An optimal real time pricing approach. Energy 2011;36(8):5374–84.

[18] Moray S, Throop N, Seryak J, Schmidt C. Energy efficiency opportunities in the stone and asphalt industry. in: Proceedings of the Twenty-Eighth Industrial Energy Technology Conference; New Orleans, Louisiana, United States; 9-12 May, 2006.

[19] De la Vergne J. Hard Rock Miner's Handbook. Arizona, United States: McIntosh Engineering Inc; 2003.

[20] Martin J, Bidarte U, Cuadrado C, Ibanez P. DSP-based board for control of jaw crushers used in mining and quarrying industry. in: Industrial Electronics Society, 2000. 26th Annual Conference of the IEEE; Nagoya, Aichi, Japan; 22–28 October, 2000.

[21] Ashok G, Denis Y. Mineral Processing Design and Operations: An Introduction. Amsterdam, Boston: Elsevier; 2006.

[22] Convey J. The milling of Canadian ores. Canada: 6th Commonwealth Mining and Metallurgical Congress; 1957.

[23] Hadjigeorgiou J, Lessard J. Numerical investigations of ore pass hang-up phenomena. International Journal of Rock Mechanics and Mining Sciences 2007;44(6):820–34.

[24] Hustrulid W. A, Bullock R. L. Underground Mining Methods: Engineering Fundamentals and International Case Studies. United States: Society for Mining, Metallurgy, and Exploration Inc.; 2001.

[25] Hadjigeorgiou J, Lessard J, Mercier-Langevin F. Ore pass practice in Canadian mines. Journal of The South African Institute of Mining and Metallurgy 2005;105(11):809–16.

[26] Esmaieli K. Stability Analysis of Ore Pass Systems at BRUNSWICK Mine. Québec, Canada: Ph.d. thesis, Facultés des Sciences et de Génie, Université Laval; 2010.

[27] Kennedy BA. Surface Mining. 2nd ed. Baltimore, Maryland, United States: Society for Mining, Metallurgy, and Exploration Inc.; 1990. p. 706-708.

[28] Pontryagin L, Boltyanskii V, Gamkrelidze R, Mishchenko E. The Mathematical Theory of Optimal Processes. New York, United States: John Wiley & Sons Inc.; 1962.

[29] Refahi A, Rezai B, Mohandesi JA. Use of rock mechanical properties to predict the Bond crushing index. Minerals Engineering 2007;20(7):662–9.

[30] Lindqvist M. Energy considerations in compressive and impact crushing of rock. Minerals Engineering 2008;21(9):631–41.

[31] Sastri S. Capacities and performance characteristics of jaw crushers. Minerals and Metallurgical Processing 1994;11(2):80–6.

[32] Roberts AW. Recent developments in feeder design and performance. Handbook of Powder Technology 2001;10:211–23, .

[33] DeDiemar R. New concepts in jaw crusher technology. Minerals Engineering 1990;3:67–74.

[34] Dunn M, Menzies I. Rockpass overview and risk assessment within the AngloGold Ashanti SA region. Journal of The South African Institute of Mining and Metallurgy 2005;105(11):753–8.

[35] Gastli A, Ahmed MM. ANN-Based Soft Starting of Voltage-Controlled-Fed IM Drive System. IEEE Transactions on Energy Conversion 2005;20(3):497–503.

Fig. 1. Typical configuration of a deep underground mine (adapted from Ref. [24]).

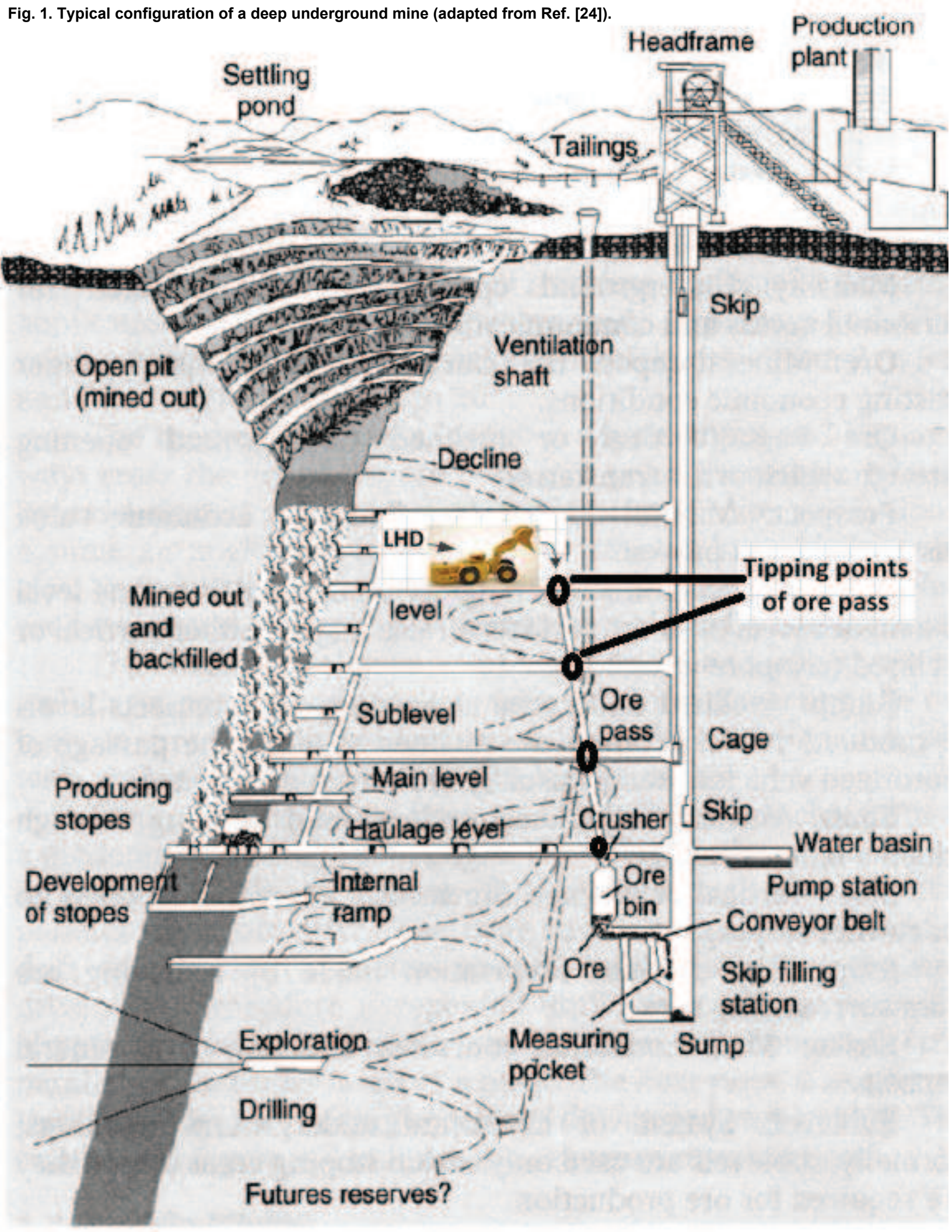

Fig. 2. Primary jaw crushing station in a deep mine.

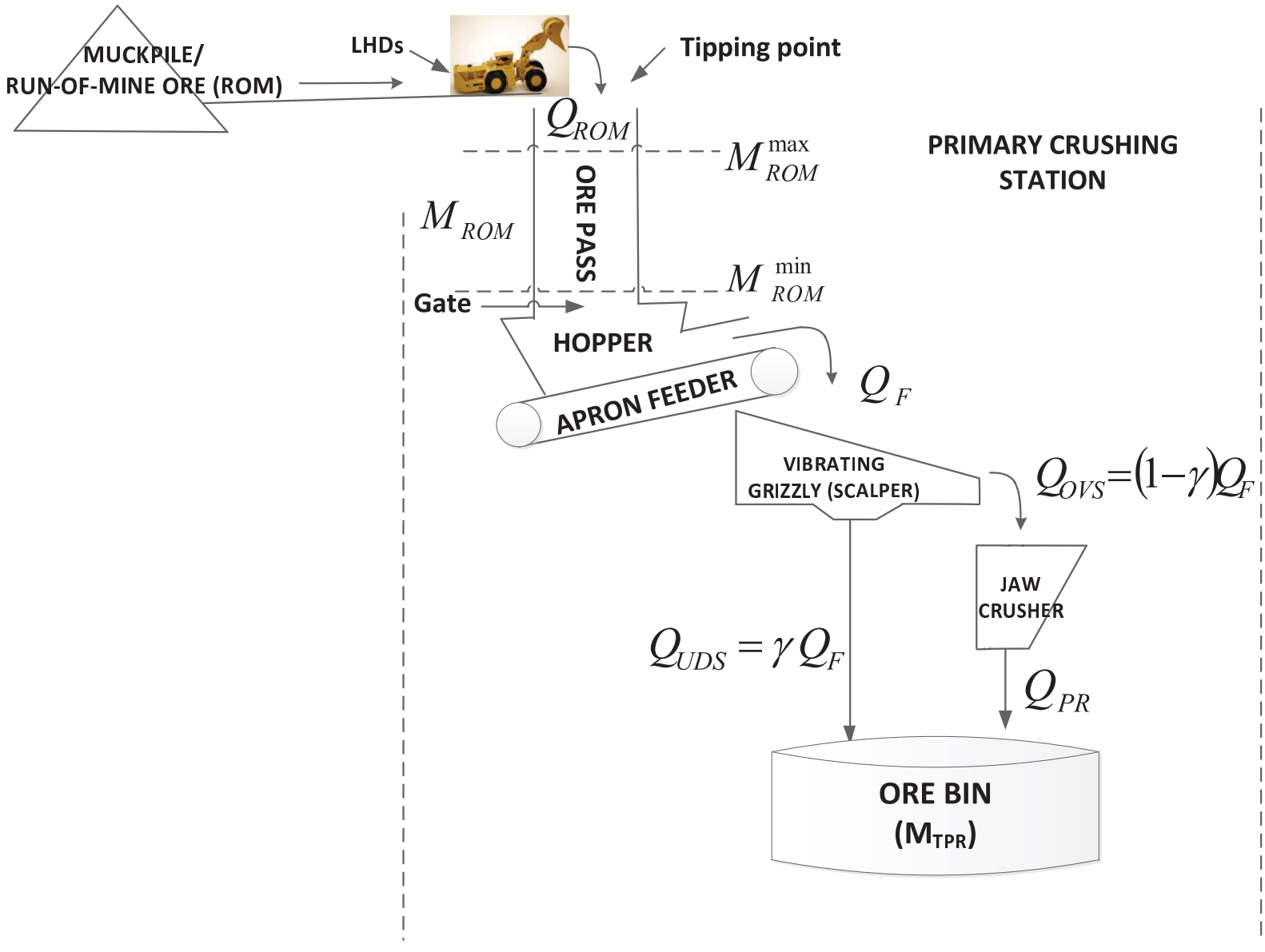

Fig. 3. Fit of throughput rate (in metric-ton/h) of C-series jaw crushers.

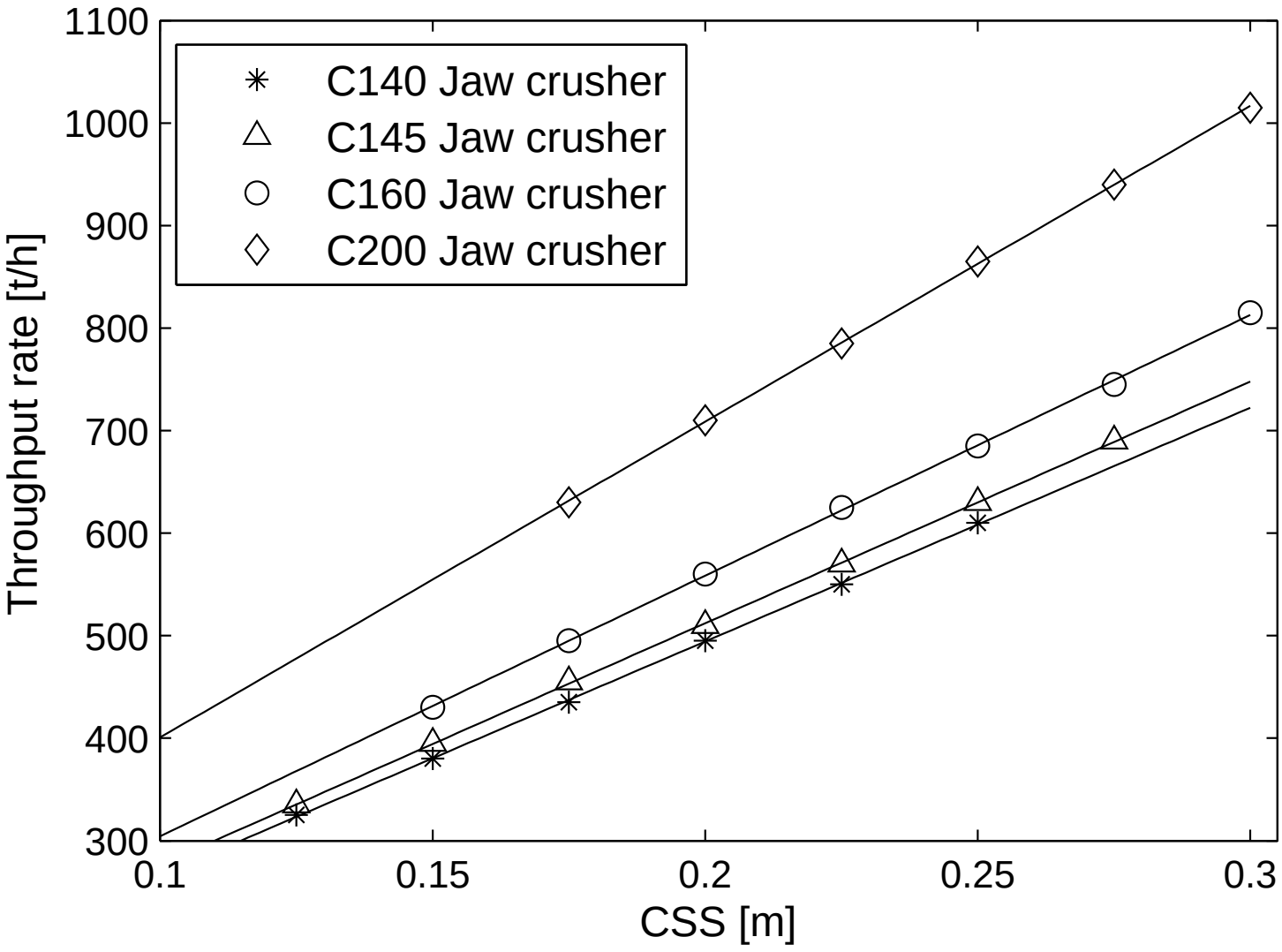

Fig. 4. VL-based optimal control and current control techniques - case I.

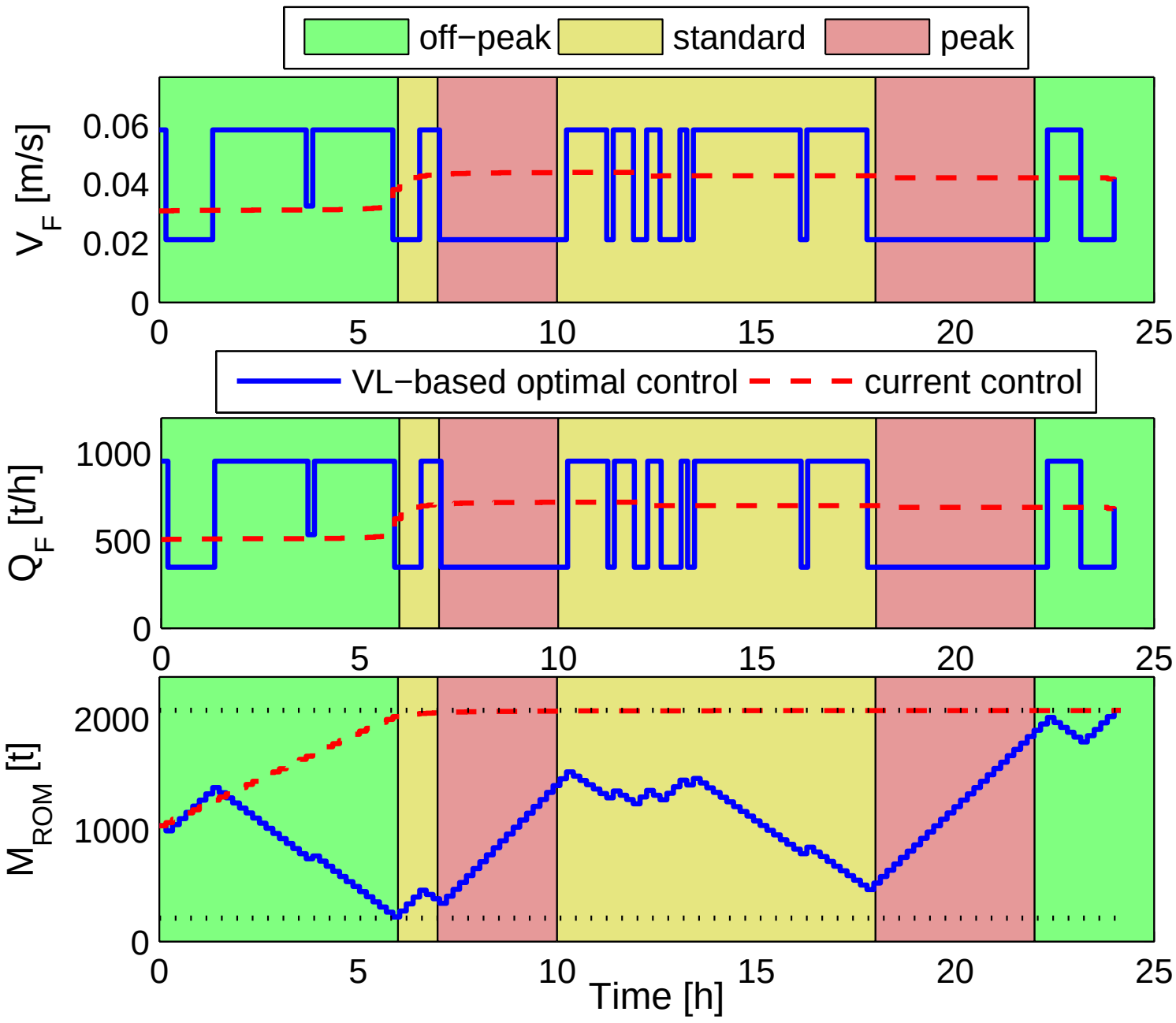

Fig. 5. VL-based optimal control and current control techniques - case I (continued).

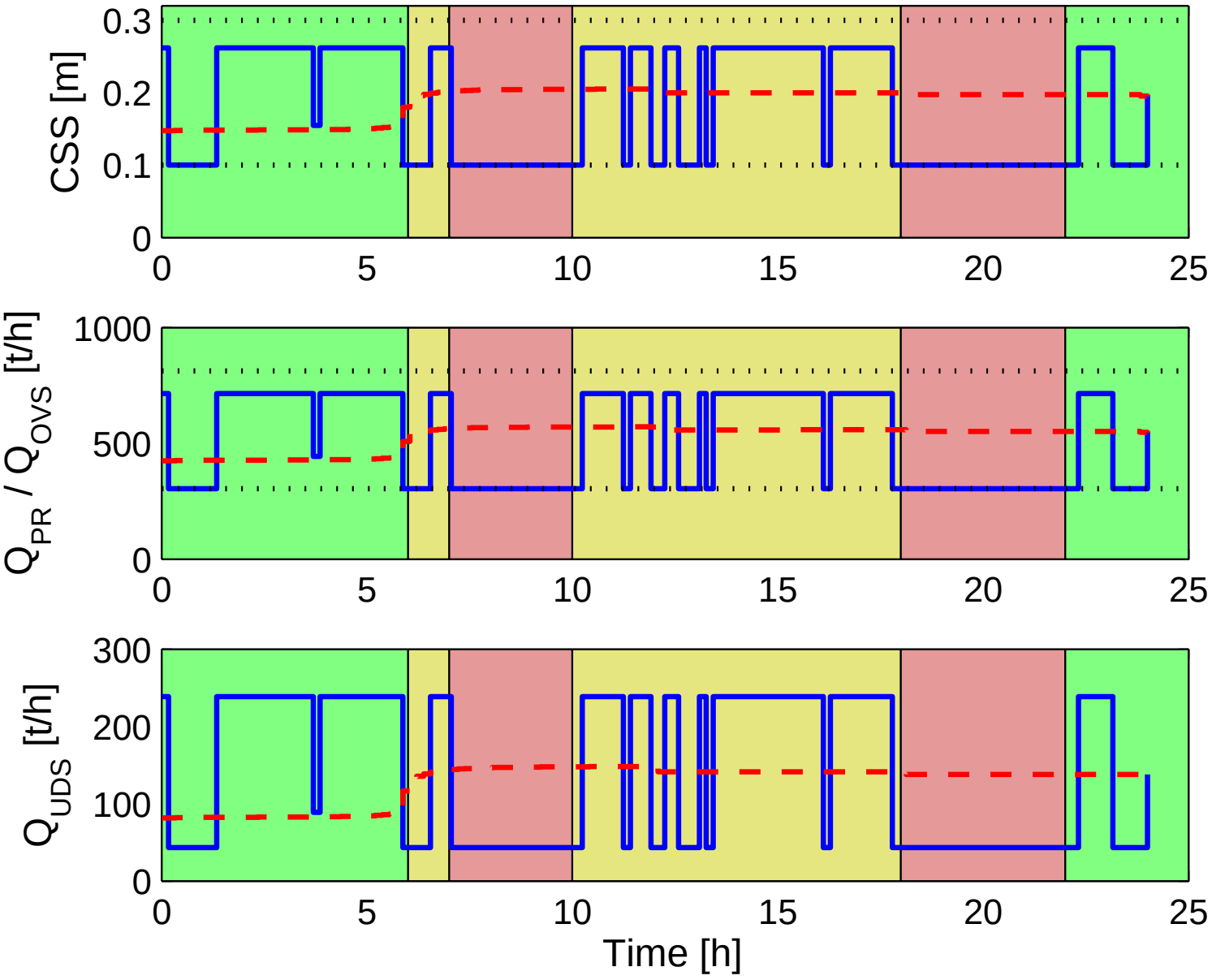

Fig. 6. Optimal switching control technique - case I.

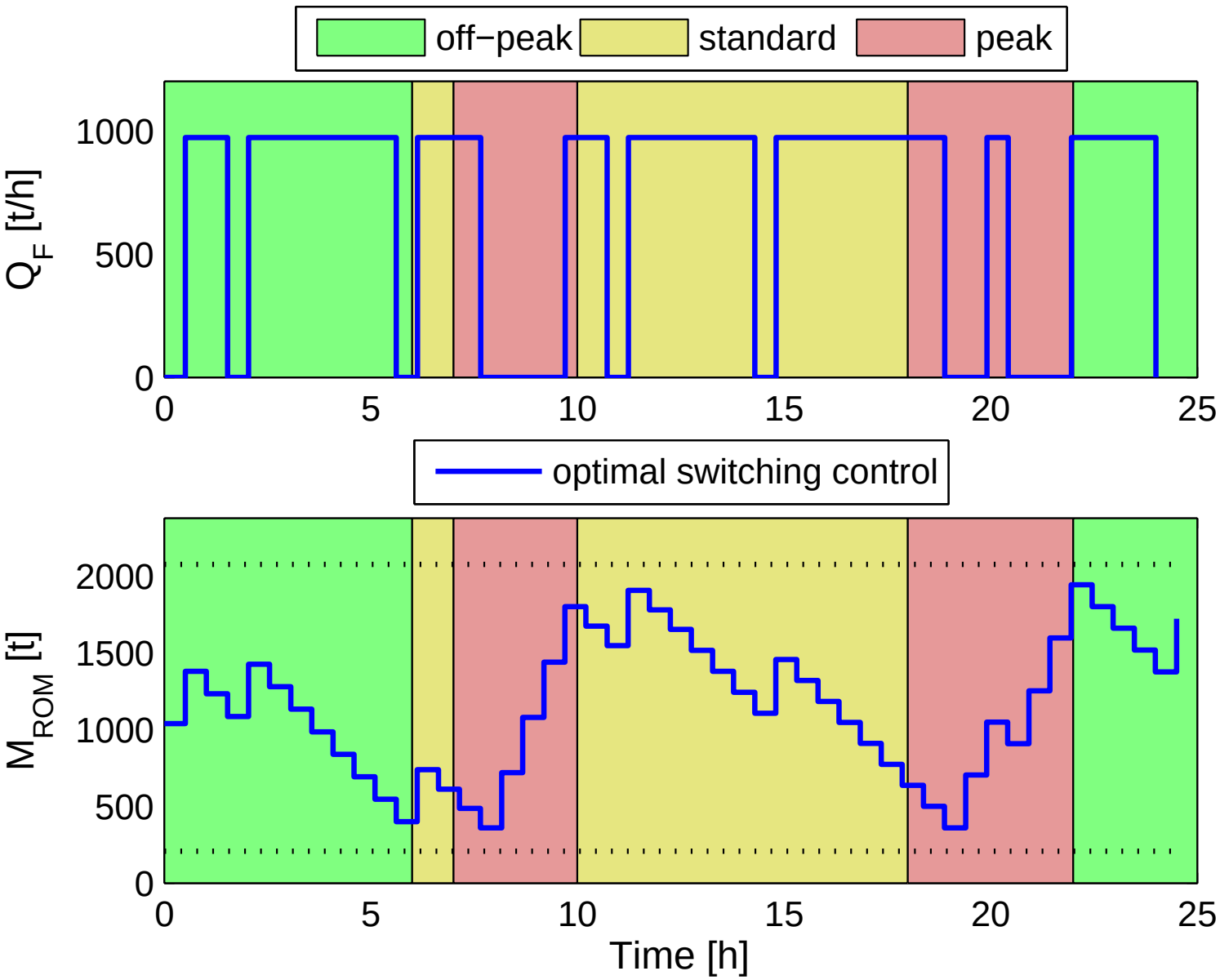

Fig. 7. VL-based optimal control and current control techniques - case II.

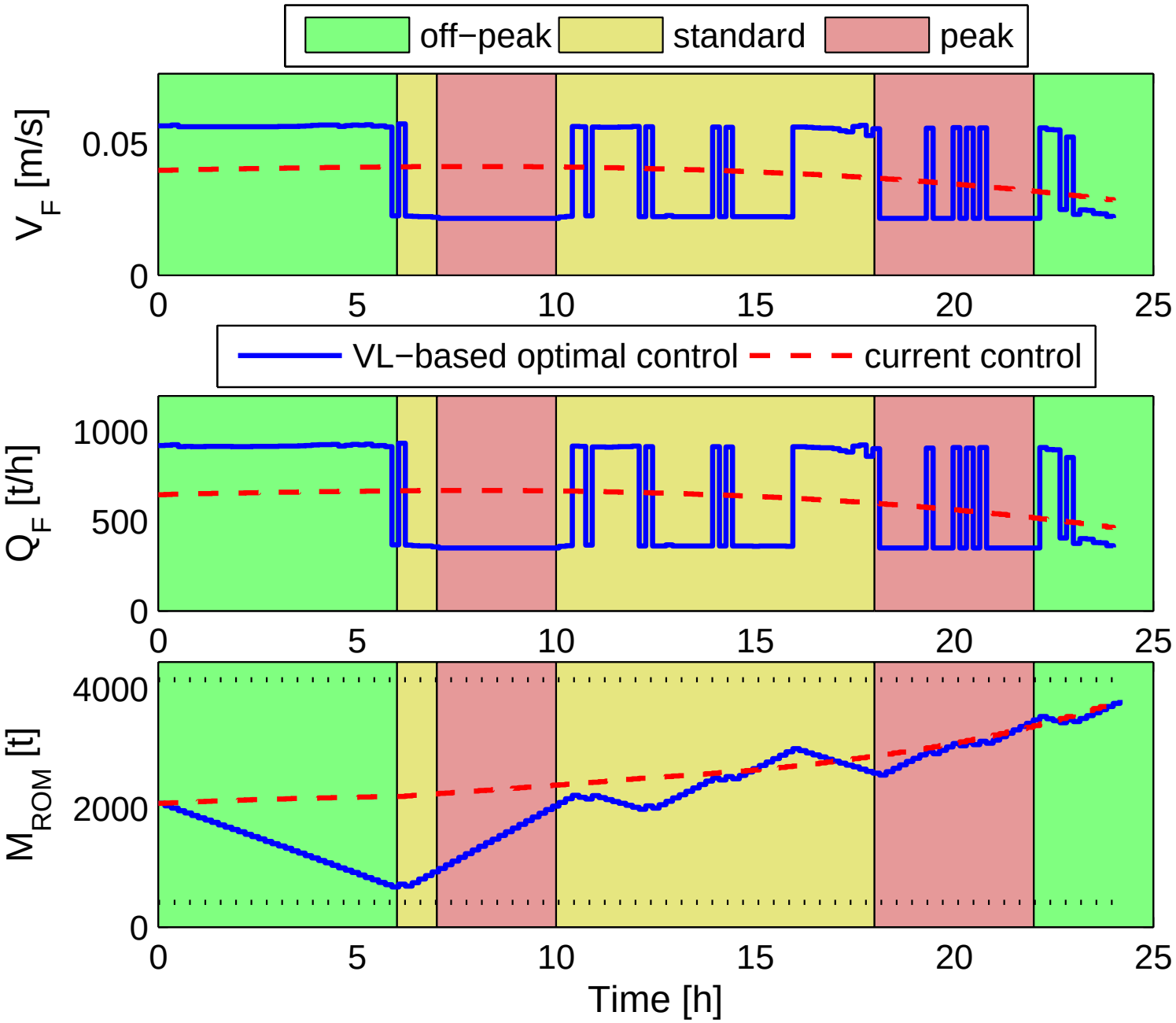

Fig. 8. VL-based optimal control and current control techniques - case II (continued).

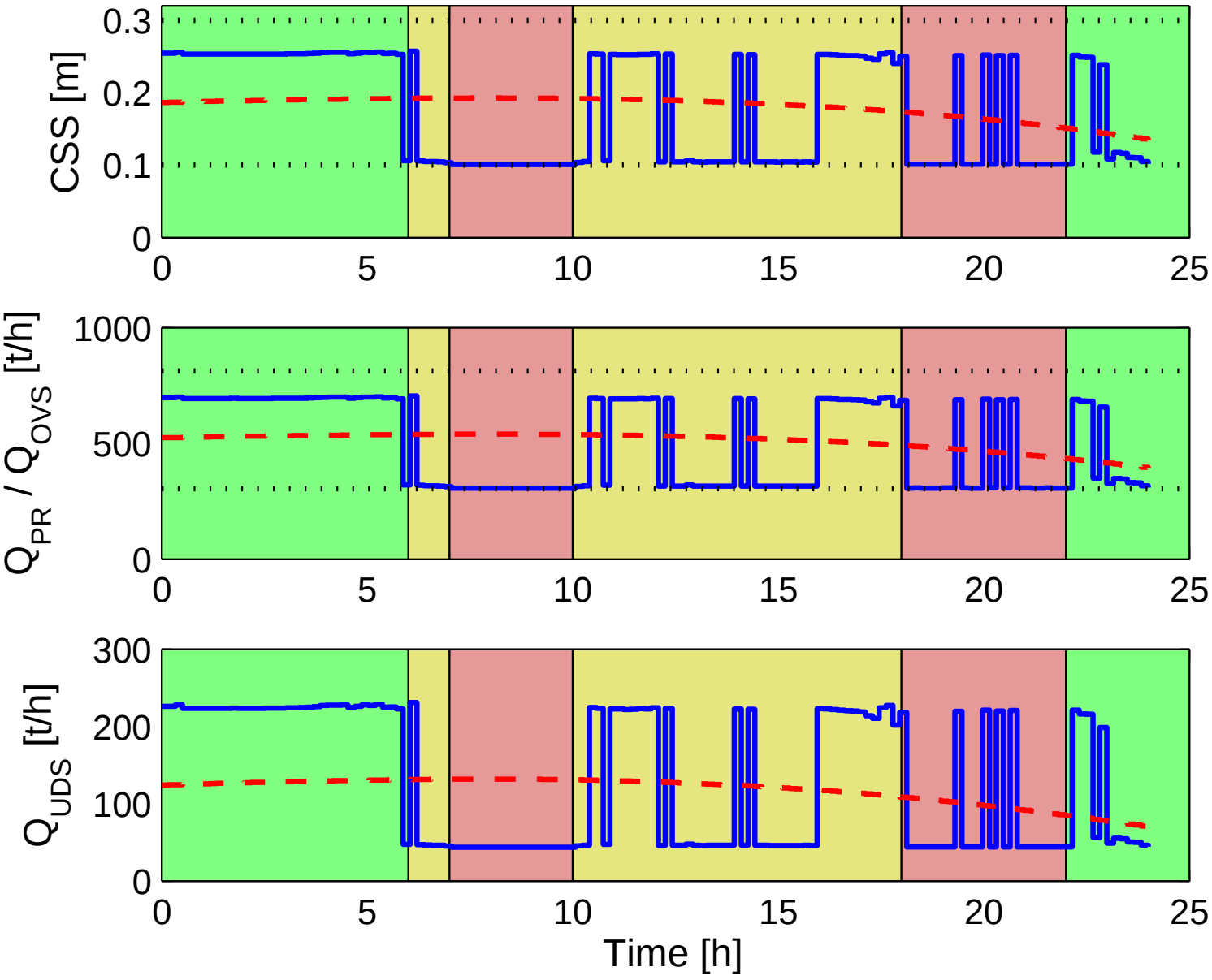

Fig. 9. Optimal switching control technique - case II.